PHYSICAL REVIEW D **88,** 074029 (2013)

Probing the Pomeron structure using dijets and γ + jet events at the LHC

C. Marquet,[1,*] C. Royon,[2,†] M. Saimpert,[2,‡] and D. Werder[3,§]

[1]*Centre de Physique Théorique, École Polytechnique, CNRS, 91128 Palaiseau, France*
[2]*IRFU/Service de Physique des Particules, CEA/Saclay, 91191 Gif-sur-Yvette Cedex, France*
[3]*Department of Physics and Astronomy, Uppsala University, Box 516, SE-751 20 Uppsala, Sweden*

(Received 20 June 2013; published 24 October 2013)

We consider hard diffractive events in proton-proton collisions at the LHC, in which both protons escape the collision intact. In such double Pomeron exchange processes, we propose to measure dijets and photon-jet final states, and we show that it has the potential to pin down the Pomeron quark and gluon contents, a crucial ingredient in the standard QCD description of hard diffraction. By comparing with predictions of the soft color interaction approach, we also show that more generally, the measurement of the photon-jet to dijet cross section ratio can put a stringent test on the QCD dynamics at play in diffractive processes in hadronic collisions.

DOI: 10.1103/PhysRevD.88.074029 PACS numbers: 13.60.Hb, 12.38.Bx, 12.38.Lg

I. INTRODUCTION

Understanding diffractive interactions in QCD has been a challenge for many years. In particular, for hard diffractive events in hadronic collisions, it seems that a description based solely on weak-coupling methods cannot be obtained. In the case of deep inelastic scattering (DIS), due to several years of experimental efforts at the Hoch Energie Ring Anlage (HERA) accelerator located at DESY, Hamburg, as well as many theoretical achievements, the situation has reached a satisfactory level. The diffractive part of the deep inelastic cross section is now well understood in perturbative QCD [1–4]. This is achieved by means of different approximation schemes each valid in their own kinematic limit. For instance, at large photon virtuality Q^2, one can use the collinear factorization of diffractive parton densities [5], while at small values Bjorken x, the nonlinear evolution of dipole scattering amplitudes is also successful [6–8]. By contrast, the description of hard diffraction in hadron-hadron collisions still poses great theoretical challenges.

Tevatron data provided evidence that, even at very large scales, collinear factorization does not apply for diffraction in hadron-hadron collisions [9]. There exist however empirical indications that the factorization breaking can be compensated by an overall factor, called the gap survival probability, independent of the details of the hard process. Nevertheless, many questions remain unanswered. Is this factor only a function of the collision energy, as often assumed? Does one need a different factor in single diffraction, double diffraction, and double-Pomeron-exchange (DPE) processes? One should be able to answer these questions at the LHC, where diffraction is a large part of the QCD program [10]. In addition, should this picture of diffraction be validated, it will be possible to further constrain the details of the theoretical description.

In this paper we focus on one aspect of this picture of diffractive events: the so-called Regge factorization of the diffractive parton densities into a Pomeron flux and Pomeron parton distributions. Such factorization is successful in DIS, but whether it also works in hadron-hadron collisions remains to be proven. In particular, the resulting Pomeron content in terms of quarks and gluons should be consistent with what has been extracted from HERA data. In order to constrain the Pomeron gluon and quark densities at the LHC, we shall consider the dijet and photon-jet processes respectively, in DPE events, meaning that both protons escape the collision intact. We show that the measurement of the photon-jet to dijet cross section ratio has the potential to pin down the Pomeron quark content, or at the very least put a stringent test on the Pomeron-like picture of diffraction.

On the contrary, a different mechanism could be responsible for diffraction in hadron-hadron collisions. For this reason, we also compare the previous expectations for the photon-jet to dijet cross section ratio in DPE processes with predictions from a different picture of diffraction, which does not invoke Pomerons nor diffractive parton distributions: the soft color interaction (SCI) model [11,12]. This approach models diffractive events exactly the same as other inelastic events, but allows for additional soft exchanges which do not significantly change the kinematics but change the color topology of the event. This changed topology can then result in rapidity gaps and leading final state protons after hadronization. In this alternative description of diffractive interactions, the QCD dynamics at play is very different compared to the more standard Pomeron picture.

The plan of the paper is as follows. In Sec. II, we present more details about the theoretical description of hard diffractive events in hadron-hadron collisions, and on their implementation into the forward physics Monte Carlo

*cyrille.marquet@cern.ch
†christophe.royon@cea.fr
‡matthias.saimpert@cea.fr
§dominik.werder@physics.uu.se

(FPMC) program, which is used in our analysis. In Sec. III, we discuss the sensitivity of the DPE dijet process to the gluon content of the Pomeron; this will be the first DPE measurement performed at the LHC. In Sec. IV, we focus on the quark content of the Pomeron, and show the improvements that can be obtained by measuring DPE photon-jet processes. Finally, in Sec. V, we compare our results with those obtained in the SCI model, for the photon-jet to dijet cross section ratio. Section VI is devoted to conclusions and outlook.

II. HARD DIFFRACTIVE PROCESSES AND THEIR IMPLEMENTATION IN FPMC

We shall focus on double Pomeron exchange processes in proton-proton collisions. The formulation of single- and double-diffractive processes is very similar, those cross sections can be obtained with simple modifications to what is presented in this section. In addition, we write our formulas for the dijet final state $J + J + X$, but they hold for the photon-jet final state $\gamma + J + X$ as well. The leading-order diagrams for those processes are pictured in Fig. 1, and the following long-distance/short-distance factorization formula is used to compute the cross sections:

$$d\sigma^{pp\to pJJXp} = \mathcal{S}_{\mathrm{DPE}} \sum_{i,j} \int d\beta_1 d\beta_2 f^D_{i/p}(\xi_1, t_1, \beta_1, \mu^2) \times f^D_{j/p}(\xi_2, t_2, \beta_2, \mu^2) d\hat{\sigma}^{ij\to JJX}, \tag{1}$$

where $d\hat{\sigma}$ is the short-distance partonic cross section, which can be computed order by order in perturbation theory (provided the transverse momentum of the jets is sufficiently large), and each factor $f^D_{i/p}$ denotes the diffractive parton distribution in a proton. These are nonperturbative objects, however their evolution with the factorization scale μ is obtained perturbatively using the Dokshitzer-Gribov-Lipatov-Altarelli-Parisi [13] evolution equations. The variables ξ and t denote, for each intact proton, their fractional energy loss and the momentum squared transferred into the collision, respectively.

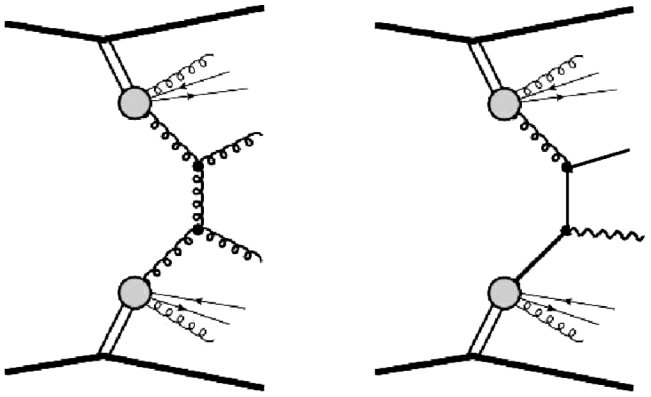

FIG. 1. Leading-order diagrams for double-Pomeron exchange dijet (left) and γ + jet (right) production in proton-proton collisions. The dijet process is sensitive to the Pomeron gluon density and the γ + jet process to the Pomeron quark densities.

Hard diffractive cross sections in hadronic collisions do not obey collinear factorization. This is due to possible secondary soft interactions between the colliding hadrons which can fill the rapidity gap(s). Formula (1) is reminiscent of such a factorization, but it is corrected with the so-called gap survival probability S which is supposed to account for the effects of the soft interactions. Since those happen on much longer time scales compared to the hard process, they are modeled by an overall factor. This is part of the assumptions that need to be further tested at the LHC. To evaluate hard cross sections in the single diffraction case, one of the diffractive parton distributions in (1) is replaced by a regular parton distribution, and the survival probability factor $\mathcal{S}_{\mathrm{SD}}$ is different as well.

To produce single diffractive and double Pomeron exchange events, FPMC uses diffractive parton distributions extracted from HERA data [14] on diffractive DIS (a process for which collinear factorization does hold). These are decomposed further into Pomeron and Reggeon fluxes $f_{\mathbb{P},\mathbb{R}/p}$ and parton distributions $f_{i/\mathbb{P},\mathbb{R}}$:

$$f^D_{i/p}(\xi, t, \beta, \mu^2) = f_{\mathbb{P}/p}(\xi, t) f_{i/\mathbb{P}}(\beta, \mu^2) + f_{\mathbb{R}/p}(\xi, t) f_{i/\mathbb{R}}(\beta, \mu^2)$$
$$\text{with} \quad f_{\mathbb{P},\mathbb{R}/p}(\xi, t) = \frac{e^{B_{\mathbb{P},\mathbb{R}} t}}{\xi^{2\alpha_{\mathbb{P},\mathbb{R}}(t)-1}}. \tag{2}$$

The diffractive slopes $B_{\mathbb{P},\mathbb{R}}$, the Regge trajectories $\alpha_{\mathbb{P},\mathbb{R}}(t) = \alpha_{\mathbb{P},\mathbb{R}}(0) + t\alpha'_{\mathbb{P},\mathbb{R}}$ and the parton densities $f_{i/\mathbb{P},\mathbb{R}}$ can be found in the literature. The secondary Reggeon contribution (with respect to the Pomeron one) has not yet been implemented in the FPMC generator but it is assumed to occur at high ξ at the edge of the forward proton detector acceptance. Obviously, it is important to measure at the LHC this contribution since the extrapolation at higher energies of the present secondary contribution performed by the H1 collaboration at HERA using the pion structure function [4] is definitely questionable. A measurement of the ξ distribution in diffractive events for dijets for instance will be of great interest since it should combine the $1/\xi$ dependence from the Pomeron part with a flatter distribution at high ξ originating from Reggeons.

Measurements at the LHC will allow one to test the validity of this further factorization of the diffractive parton distributions into a Pomeron flux and Pomeron parton distributions, as well as the universality of those Pomeron fluxes and parton distributions. Finally, for those processes in which the partonic structure of the Pomeron is probed, the existing HERWIG matrix elements of inelastic production are used in FPMC to calculate the partonic cross sections, at leading order.

III. SENSITIVITY TO THE POMERON STRUCTURE IN GLUONS

In this section, we detail the potential measurements to be performed at the LHC in order to constrain the gluon structure in the Pomeron. We will start by describing the experimental framework (the proton detectors to be installed especially in the CMS and ATLAS experiments) and the Monte Carlo tools. We will finish the section by giving the potential observables which will allow one to constrain the gluon content inside the Pomeron.

A. Experimental framework

In the following, we assume the intact protons to be tagged in the forward proton detectors to be installed by the CMS/Totem and the ATLAS collaborations [10]. Two different places at 210–220 and 420 m in the LHC can be used to install such detectors. The idea is to measure scattered protons at very small angles at the interaction point and to use the LHC magnets as a spectrometer to detect and measure the intact protons. In the following, we choose as an example the acceptances of the forward detectors to be installed in the ATLAS collaboration at 210 and 420 m:

(i) $0.015 < \xi < 0.15$ for 210 m detectors only,
(ii) $0.0015 < \xi < 0.15$ for a combination of 210 and 420 m detectors,

knowing the fact that the acceptance for such detectors in CMS-Totem is similar.

In order to produce double Pomeron exchange events, where both protons are intact in the final state, and produce all studies mentioned in this paper we use the forward physics Monte Carlo (FPMC) generator [15]. FPMC aims to accommodate all relevant models for forward physics which could be studied at the LHC and contains in particular the two-photon and double Pomeron exchange processes. The generation of the forward processes is embedded inside HERWIG [16]. The great advantage of the program is that all processes with leading protons can be studied in the same framework, using the same hadronization model.

B. Measurement of the dijet cross section and constraints on the gluon density in the Pomeron

The dijet production in DPE events at the LHC is sensitive to the gluon density in the Pomeron. The aim of this section is to study if we can constrain further the gluon density in the Pomeron compared to the determination at HERA and to check if the Pomeron model is universal between HERA and LHC. In order to quantify how well we are sensitive to the Pomeron structure in terms of gluon density at the LHC, we display in Fig. 2, left, the dijet cross section as a function of the jet p_T. The central black line displays the cross section value for the gluon density in the Pomeron measured at HERA including an additional survival probability of 0.03. The yellow band shows the effect of the 20% uncertainty on the gluon density taking into account the normalization uncertainties. The dashed curves display how the dijet cross section at the LHC is sensitive to the gluon density distribution especially at high β. For this sake, we multiply the gluon density in the Pomeron from HERA by $(1-\beta)^{\nu}$ where ν varies between -1 and 1. When ν is equal to -1 (respectively 1), the gluon density is enhanced (respectively decreased) at high β. From Fig. 2, we notice that the dijet cross section is indeed sensitive to the gluon density in the Pomeron and we can definitely check if the Pomeron model from HERA and its structure in terms of gluons is compatible between HERA and the LHC. This will be an important test of the Pomeron universality. This measurement can be performed for a luminosity as low as 10 pb^{-1} since the cross section is very large (typically, one day at low luminosity without pileup at the LHC). It is worth noticing that this measurement will be limited by systematic uncertainties

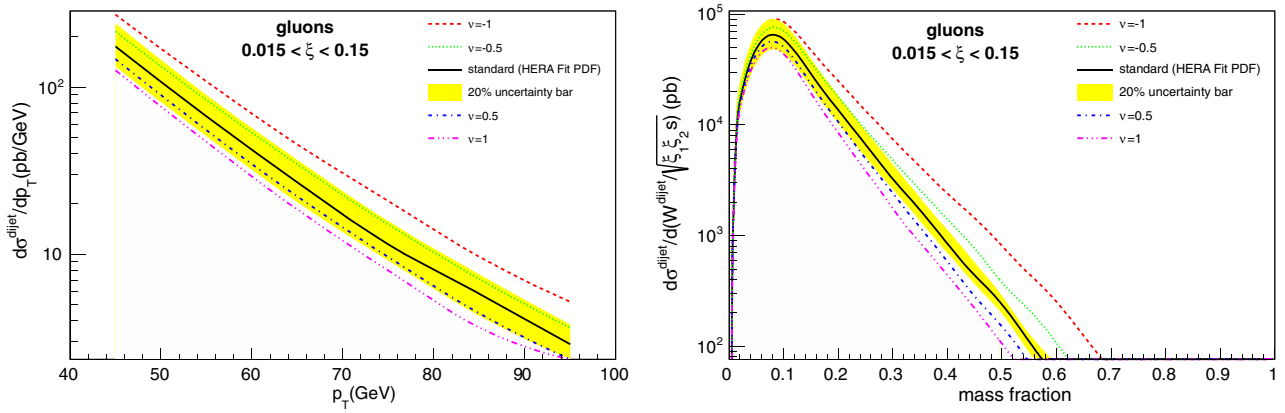

FIG. 2 (color online). Left: DPE dijet cross section as a function of jet p_T at the LHC. Right: DPE dijet mass fraction distribution. The different curves correspond to different modifications of the Pomeron gluon density extracted from HERA data (see text).

(not the statistical ones). Typically, if the jet energy scale is known with a precision of 1%, we expect the systematics on the jet cross section mainly due to jet energy scale and jet p_T resolution to be of the order of 15%.

However, from this measurement alone, it will be difficult to know if the potential difference between the expectations from HERA and the measurement at the LHC is mainly due to the gluon density or the survival probability since the ratio between the curves for the different gluons (varying the ν parameters) is almost constant. It will be difficult to know if these effects are rather due to the value of the survival probability.

An additional observable more sensitive to the gluon density in the Pomeron is displayed in Fig. 2, right. This is the so-called dijet mass fraction, the ratio of the dijet mass to the total diffractive mass computed as $\sqrt{\xi_1 \xi_2 S}$, where $\xi_{1,2}$ are the proton fractional momentum carried by each Pomeron and S the center-of-mass energy of 14 TeV. We note that the curves corresponding to the different values of ν are much more spaced at high values of the dijet mass fraction, meaning that this observable is indeed sensitive to the gluon density at high β. This is due to the fact that the dijet mass fraction is equal to $\sqrt{\beta_1 \beta_2}$, where $\beta_{1,2}$ are the Pomeron momentum fraction carried by the parton inside the Pomeron which interacts. The measurement of the dijet cross section as a function of the dijet mass fraction is thus sensitive to the product of the gluon distribution taken at β_1 and β_2. It is worth mentioning that exclusive dijet events will contribute to this distribution at higher values of the dijet mass fraction above 0.6–0.7 [17].

Once the gluon distribution in the Pomeron will be constrained at the LHC using dijet events and the measurement of the dijet mass fraction, it is possible to constrain further the quark content inside the Pomeron.

IV. SENSITIVITY TO THE POMERON STRUCTURE IN QUARKS USING γ + jet EVENTS

In this section, we detail the potential measurements to be performed at the LHC in order to constrain for the first time the quark structure in the Pomeron.

Figure 3 displays the γ + jet and dijet cross sections as a function of the d/u quark content of the Pomeron for two different acceptances in ξ for the forward detectors, $0.015 < \xi < 0$, 15 (left) and $0.0015 < \xi < 0.15$ (right), while keeping $u + d + s$ constant. The γ + jet cross section varies by about a factor 2.5 when u/d changes, while the dijet cross section remains constant since it originates from gluon exchanges. As expected, the cross section for γ + jet events is much smaller and will limit the statistics of the measurement. We note that a luminosity of 200–300 pb^{-1} is needed to perform the measurement with enough statistics when the proton is detected in ATLAS Forward Physics project (AFP). The main limiting factor is obviously the AFP acceptance since the diffractive mass has to be larger than 350 GeV for 210 m detectors and about 100 GeV for 210 and 420 m detectors together. However, we will notice in the following that detecting both protons is crucial for this measurement. Figure 4 displays the γ + jet to the dijet cross section ratio as a function of the d/u quark content in the Pomeron for two different acceptances in ξ corresponding to the 210 and 210/420 m detectors. Measuring ratios is definitely better since most of the systematics uncertainties will cancel. As expected, the ratios vary by a factor 2.5 following the assumptions on u/d in the proton.

Figures 5 and 6 display possible observables at the LHC that can probe the quark content in the Pomeron. Figure 5 displays the γ + jet to the dijet cross section ratios as a function of the leading jet p_T for different assumptions on the quark content of the Pomeron, d/u varying between 0.25 and 4 in steps of 0.25. We notice that

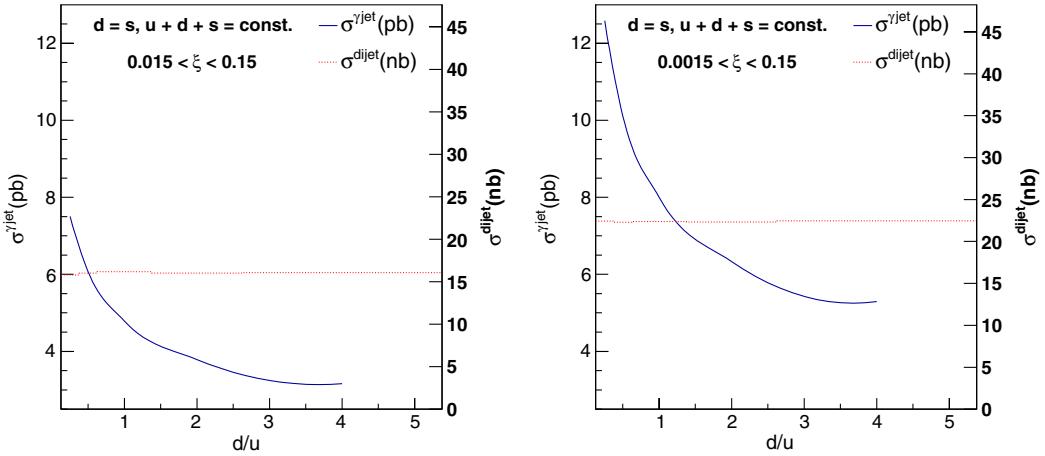

FIG. 3 (color online). DPE γ + jet and dijet cross section as a function of d/u, reflecting the Pomeron quark flavor composition. Left: acceptance of the 210 m proton detectors. Right: acceptance of both the 210 and 420 m detectors.

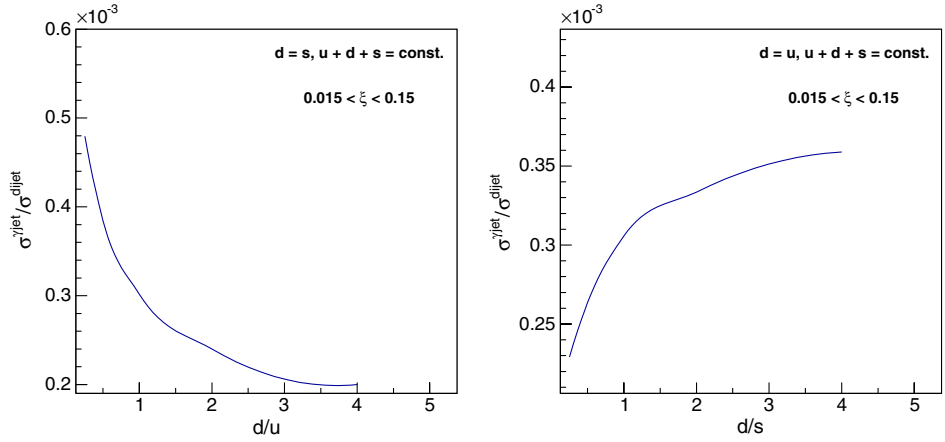

FIG. 4 (color online). DPE γ + jet to dijet cross section ratio, for the acceptance of the 210 m proton detectors. Left: as a function of d/u. Right: as a function of d/s.

the cross section ratio varies by a factor 2.5 for different values of u/d and the ratio depends only weakly on the jet p_T except at low values of jet p_T, which is due to the fact that we select always the jet with the highest p_T in the dijet cross section (and this is obviously different for the γ + jet sample where we have only one jet most of the time). The aim of the jet p_T distribution measurement is twofold: is the Pomeron universal between HERA and the LHC and what is the quark content of the Pomeron? As it was mentioned in Sec. II, the QCD diffractive at HERA assumed that $u = d = s = \bar{u} = \bar{d} = \bar{s}$, since data were not sensitive to the difference between the different quark component in the Pomeron. The LHC data will allow us to determine for instance which value of d/u is favored by data. Let us assume that $d/u = 0.25$ is favored. If this is the case, it will be needed to go back to the HERA QCD diffractive fits and check if the fit results at HERA can be modified to take into account this assumption. If the fits to HERA data lead to a large χ^2, it would indicate that the Pomeron is not the same object at HERA and the LHC. On the other hand, if the HERA fits work under this new assumption, the quark content in the Pomeron will be further constrained. The advantage of measuring the cross section ratio as a function of jet p_T is that most of the systematic uncertainties due to the determination of the jet energy scale will cancel. This is however not the case for the jet energy resolution since the jet p_T distributions are different for γ + jet and dijet events.

Figure 6 displays the γ + jet to dijet cross section ratio as a function of the diffractive mass M computed from the proton ξ measured in the forward detectors $M = \sqrt{\xi_1 \xi_2 S}$ where ξ_1 and ξ_2 are the momentum fraction of the proton carried by each Pomeron and measured in the proton detectors. The advantage of this variable is that most of systematic uncertainties due to the measurement of the diffractive mass cancel since the mass distributions for γ + jet and dijet are similar (see Fig. 7). The typical resolution on mass is in addition very good of the order of 1% to 2%. The statistical uncertainties corresponding to 300 pb^{-1}, three weeks of data taking at low pileup, are also shown on the figure. This measurement will be fundamental to constrain in the most precise way the Pomeron structure in terms of quark densities, and to test the Pomeron universality between the Tevatron and the LHC.

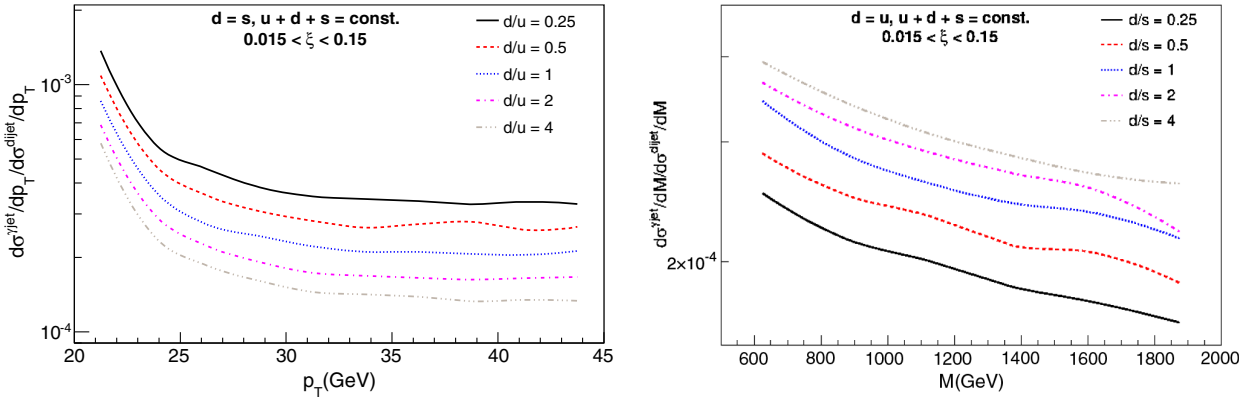

FIG. 5 (color online). DPE γ + jet to dijet differential cross section ratio, for the acceptance of the 210 m proton detectors. Left: as a function of jet p_T, for different values of d/u. Right: as a function of the diffractive mass M, for different values of d/s.

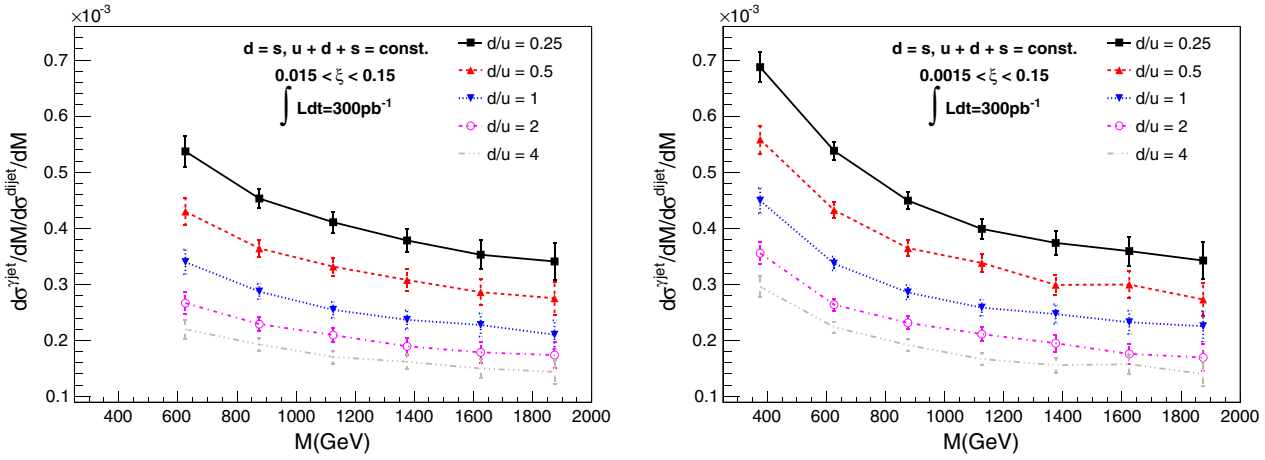

FIG. 6 (color online). DPE γ + jet to dijet differential cross section ratio as a function of the diffractive mass M, for different values of d/u. Left: acceptance of the 210 m proton detectors. Right: acceptance of both the 210 and 420 m detectors.

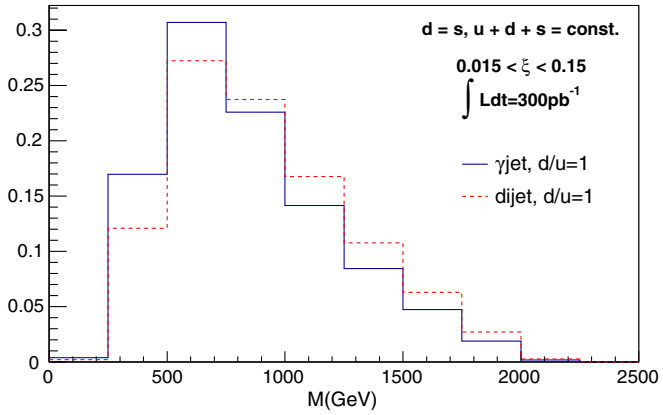

FIG. 7 (color online). Distribution (normalized to 1) of the total diffractive mass ($M = \sqrt{\xi_1 \xi_2 S}$) for DPE production of dijets (dashed line, right scale) and γ + jet events (full line, left scale). Since the distributions are similar the systematics uncertainties and the resolution effects will almost cancel in the cross section ratio.

Let us notice that the measurement can be performed with 100 pb^{-1} (about one week of data taking), but this would increase the statistical uncertainties in Fig. 6 of about 40%. It would still be possible to distinguish between extreme models. 300 pb^{-1} is the optimal luminosity for this measurement in order to get a more precise measurement. Working at higher pileup will require new strategies to be developed:

(i) the measurement of the time of flight of the protons using dedicated timing detectors will allow us to know if the protons originate from the same vertex as the gamma + jet event. Typically, for a pileup of 3, and a timing detector resolution of the order of 20 ps, the background can be reduced to a negligible value.

(ii) even if it is less probable that the photon originates from a pileup event, it is possible to check this by measuring the cross section for photon inducing lepton pairs. For instance, the probability of a photon to give a lepton pair due to dead material in ATLAS is of the order of 60% for medium photon pT.

V. COMPARISON WITH SOFT COLOR INTERACTION MODELS

A. Soft color interaction models

Soft color interaction models (SCI) describe [11,12] additional interactions between colored partons below the conventional cutoff for perturbative QCD. These are based on the assumption of factorization between the conventional perturbative event and the additional nonperturbative soft interactions. Soft exchanges imply that the changes in momenta due to the additional exchanges are very small, whereas the change in the event's color topology due to exchanges of color charge can lead to significant observables, e.g. rapidity gaps and leading beam remnants. The probability to obtain a leading proton at the LHC in the context of SCI models depends on the color charge and the kinematic variables of the beam remnant before hadronization. In string hadronization models, a colored remnant will be modeled as an end point of a string, and the hadronization procedure will cause the momentum of the beam remnant to be most likely distributed between multiple hadrons, so that a leading beam remnant on parton level will not be turned into a single leading hadron. On the other hand, a color-singlet remnant on parton level can be mapped on a single leading hadron if the kinematics allow it. To obtain a single leading proton within SCI models, the beam remnant may therefore not be disturbed too much by the perturbative part of the event, i.e. $\sqrt{t} \sim \Lambda_{\mathrm{QCD}}$. This is seen as the typical experimentally observed distribution of e^{-bt} with $b \sim (2\Lambda^2_{\mathrm{QCD}})^{-1} \sim 7\,\mathrm{GeV}^{-2}$.

A main conceptual difference between the DPE and SCI models is that the SCI model treats "diffractive" and "nondiffractive" events on equal footing. This implies in particular that an event sample based on a later cut in ξ of the proton's momentum loss can also include events where

the beam remnant was not a color singlet on parton level but where the cut in ξ was fulfilled by a leading proton from string hadronization. Figure 9 shows the distribution of events in the fractional momentum loss ξ of the proton on a single side for dijet events with $p_T > 20$ GeV. The distribution shows the increase in cross section for very small momentum losses of the beam protons, typical for diffractive scattering. In order to compare [18] with models which describe diffractive scattering in terms of a Pomeron without additional Reggeons, we therefore constrain the analysis to the region of phase space where the momentum loss of the leading final state protons is very small, so that the background due to nondiffractive events, which would not be accounted for by a purely Pomeron based model, can be neglected.

B. γ + jet over jet + jet ratio from SCI

In order to compare SCI- and Pomeron-like models, we request in the following $\xi \leq 0.02$ for the protons on both sides to stay in the region of the diffractive peak in the SCI model, even though a comparison with the ξ distribution from CDF [19] shows that the transition to a diffractive sample may be defined already at larger values of ξ up to about 0.1. An example for a basic process contributing to the γ + jet cross section is depicted in Fig. 8, where on both sides a gluon is resolved in the proton. While one gluon can be directly connected to the hard matrix element, the other gluon fluctuates in this example into a $q\bar{q}$ pair, giving the quark for the hard process. This illustrates another difference between the models, which is the QCD evolution of the initial state, treated like in standard nondiffractive processes, whereas the HERWIG/DPE model describes the process by a hard matrix element which resolves the content of the Pomeron. As before, we require in addition to the leading protons $p_T > 20$ GeV for the jets and the γ, and $|\eta| < 4.4$. These requirements translate for a central event at LHC 14 TeV to a minimum $\xi \simeq 2.9 \times 10^{-3}$. Predictions for the γ + jet and jet + jet cross sections are obtained from PYTHIA 6.4 [20] plus SCI with jet reconstruction via an anti-k_T algorithm [21] with radius parameter $R = 0.6$. The contributing hard matrix

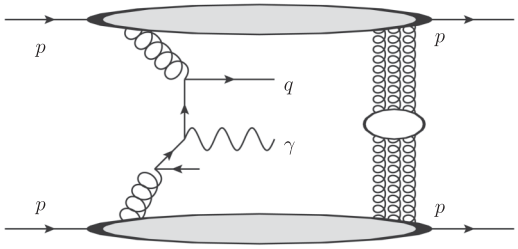

FIG. 8. γ + jet production described in terms of SCI. This example depicts the case of two resolved gluons in the protons, one of which branches into a $q\bar{q}$ pair, described by initial state radiation in a Monte Carlo program. The matrix element for $qg \to q\gamma$ is in the center. Additional soft color exchanges are depicted at the right end.

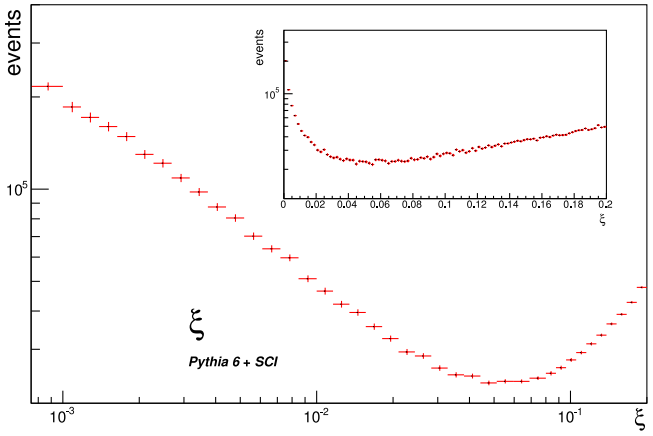

FIG. 9 (color online). Distribution in ξ of forward protons at pp 14 TeV for the SCI model requiring dijets with $p_T > 20$ GeV. Kinematic cuts for comparison between PYTHIA/SCI and HERWIG/DPE chosen such that the event sample is dominated by diffractive forward contribution.

elements for events passing the cuts are for the γ + jet cross section $fg \to f\gamma$ (90%) and $f\bar{f} \to g\gamma$ (5%), and for the jet + jet cross section $gg \to gg$ (50%), $fg \to fg$ (38%), $gg \to f\bar{f}$ (8%), and $f\bar{f} \to f\bar{f}$ ($\sim 2\%$). We compare in Figs. 10 and 11 the ratios of γ + jet and jet + jet as distributions in the p_T of the leading jet, and in diffractive mass $\sqrt{\hat{s}}$ based on the leading protons. We note first the overall quite good agreement between both models, which is remarkable especially because the SCI model's parameters do not change between HERA, Tevatron and LHC, and because PYTHIA/SCI uses the standard proton PDF without further modifications. Figure 10 suggests best agreement of the HERWIG/DPE model with PYTHIA/SCI for $d/u \simeq 1$. Figure 11 shows that the models predict different ratios of the cross sections when approaching smaller $\sqrt{\hat{s}}$. In the case of HERWIG/DPE, the ratio increases significantly towards smaller values of $\sqrt{\hat{s}}$, whereas it is less dependent on $\sqrt{\hat{s}}$ for the case of PYTHIA/SCI within the range of $\xi < 0.02$ under consideration. Allowing a more loose cut $\xi < 0.03$,

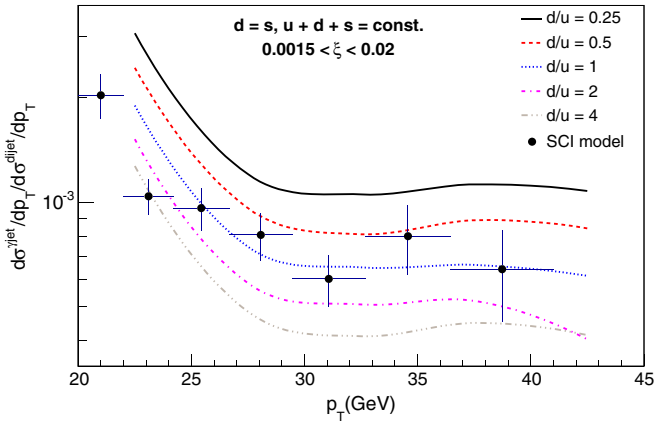

FIG. 10 (color online). Ratio of γ + jet over jet + jet cross section differential in the highest p_T jet.

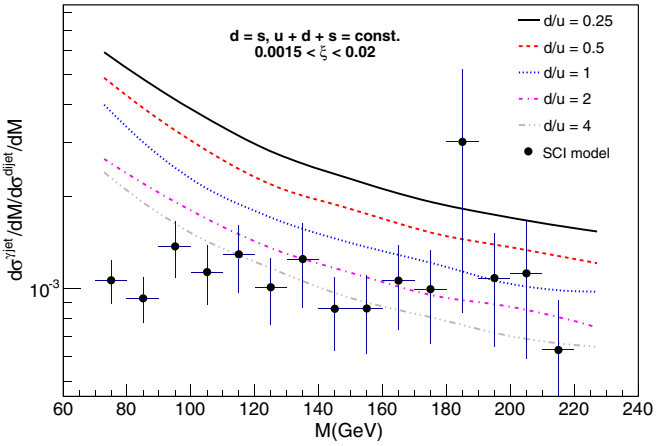

FIG. 11 (color online). Ratio of γ + jet over jet + jet cross section differential in the total diffractive mass $\sqrt{\hat{s}} = \sqrt{s\xi_1\xi_2}$ given by the leading protons.

the ratio $R(\sqrt{\hat{s}})$ at a somewhat larger value of $\sqrt{\hat{s}}$ behaves as $R(100\ \text{GeV})/R(400\ \text{GeV}) \simeq 1.8$ showing a slow decrease with p_T. By measuring the distribution of the γ + jet to the dijet cross section ratio, it will be possible to distinguish for the first time between SCI/PYTHIA and DPE/HERWIG models using in particular the slope of the diffractive mass distribution. Let us note further that the MC predictions depend also on the specific tune of the Monte Carlo and we indeed test the prediction of the model as implemented in a Monte Carlo. In addition, it is worth noticing that the comparison between both models can surely be accomplished up to $\xi \sim 0.1$ (if we follow the CDF data) and thus in the acceptance of the 210 m forward proton detectors.

VI. CONCLUSION

The measurement of diffractive processes at the LHC will allow us to get a better understanding of the Pomeron. The dijet cross section measured with a luminosity of 10 pb^{-1} (one day of data taking at low luminosity at the LHC) increases our knowledge on the gluon content in the Pomeron and allows us to further test whether the Pomeron is different at ep and pp colliders, which is a fundamental theoretical question. This measurement will be made possible by the installation of forward proton detectors located at about 210 m (and 420 m) from the interaction point of the ATLAS and CMS collaborations.

The measurement of the ratio of the γ + jet to the dijet cross section allows us to assess directly the quark content of the Pomeron (let us recall that present QCD fits assume $u = \bar{u} = d = \bar{d} = s = \bar{s}$) and again to compare the structure of the Pomeron at ep and pp colliders in addition of constraining the quark structure in the Pomeron. The best observable is the total diffractive mass obtained from the reconstruction of the proton momentum loss measured in the forward proton detectors, since most of the systematics disappear in the ratio of the γ + jet to the dijet cross sections.

In addition, diffractive processes with two identified leading outgoing protons allows us to test the predictions of soft color exchange models at unprecedented center-of-mass energies. We find an overall good agreement between HERWIG/DPE and PYTHIA/SCI for the prediction of the ratio between γ + jet and jet + jet cross sections, but the distribution of this ratio as a function of the total diffractive mass distributions may allow one to distinguish between the HERWIG/DPE and PYTHIA/SCI models because the latter leads to a more flat dependence on the total diffractive mass, giving further insight into soft QCD.

Another possibility to constrain the Pomeron structure would be to use Z + jet and W + jet events. The Z + jet cross section is typically 10 times lower than the γ + jet one, making it impossible to measure it without pileup. In addition, the Z boson must decay leptonically in order to get a reasonable background, which gives a branching ratio of the order of 10%. The timing detector will be fundamental in order to perform that measurement in a moderate pileup environment. For an average pileup of 20 per bunch crossing, one week of data corresponds to about 2 fb^{-1}. This means that this measurement would require at least 3 or 4 weeks at this kind of pileup. The measurement of W + jet would require the same kind of luminosity.

ACKNOWLEDGMENTS

We thank G. Ingelman, O. Kepka, M. Mangano, and R. Peschanski for discussions and comments.

[1] S. Chekanov *et al.* (ZEUS Collaboration), Nucl. Phys. **B800**, 1 (2008).
[2] S. Chekanov *et al.* (ZEUS Collaboration), Nucl. Phys. **B816**, 1 (2009).
[3] F. D. Aaron, C. Alexa, V. Andreev, S. Backovic, A. Baghdasaryan, E. Barrelet, W. Bartel, K. Begzsuren *et al.*, Eur. Phys. J. C **71**, 1578 (2011).
[4] F. D. Aaron *et al.* (H1 Collaboration), Eur. Phys. J. C **72**, 2074 (2012).
[5] J. C. Collins, Phys. Rev. D **57**, 3051 (1998); **61**, 019902(E) (1999).
[6] K. J. Golec-Biernat and M. Wusthoff, Phys. Rev. D **60**, 114023 (1999).
[7] Y. V. Kovchegov and E. Levin, Nucl. Phys. **B577**, 221 (2000).
[8] C. Marquet, Phys. Rev. D **76**, 094017 (2007).
[9] T. Affolder *et al.* (CDF Collaboration), Phys. Rev. Lett. **84**, 5043 (2000).

[10] ATLAS Collaboration, Report No. CERN-LHCC-2011-012.
[11] A. Edin, G. Ingelman, and J. Rathsman, Phys. Lett. B **366**, 371 (1996); Z. Phys. C **75**, 57 (1997).
[12] J. Rathsman, Phys. Lett. B **452**, 364 (1999).
[13] G. Altarelli and G. Parisi, Nucl. Phys. **B126**, 298 (1977); V. N. Gribov and L. N. Lipatov, Sov. J. Nucl. Phys. **15**, 438 (1972); **15**, 675 (1972); Y. L. Dokshitzer, Sov. Phys. JETP **46**, 641 (1977).
[14] A. Aktas *et al.* (H1 Collaboration), Eur. Phys. J. C **48**, 715 (2006).
[15] M. Boonekamp, A. Dechambre, V. Juranek, O. Kepka, M. Rangel, C. Royon, and R. Staszewski, arXiv:1102.2531.
[16] G. Corcella, I. G Knowles, G. Marchesini, S. Moretti, K. Odagiri, P. Richardson, M. H. Seymour, and B. R Webber, J. High Energy Phys. 01 (2001) 010.
[17] O. Kepka and C. Royon, Phys. Rev. D **76**, 034012 (2007).
[18] G. Ingelman, R. Pasechnik, J. Rathsman, and D. Werder, Phys. Rev. D **87**, 094017 (2013).
[19] T. Aaltonen *et al.* (CDF Collaboration), Phys. Rev. D **86**, 032009 (2012).
[20] T. Sjostrand, S. Mrenna, and P. Z. Skands, J. High Energy Phys. 05 (2006) 026.
[21] M. Cacciari, G. P. Salam, and G. Soyez, J. High Energy Phys. 04 (2008) 063.